Continuing Education Series

Cardiovascular SPECT

Russell Folks, Lawrence Banks, Michael Plankey, Jennifer A. Mattera, Robin A. Greene, Kirk D. Brust, Michael M. Graham, and Gary R. Caputo

Emory University Hospital, Atlanta, Georgia; Yale-New Haven Hospital, New Haven, Connecticut; and University of Washington School of Medicine, Seattle, Washington

This is the third continuing education article in a series on SPECT imaging. After reading and studying this article, the reader should be able to discuss the SPECT procedures described for evaluation of the heart, including the advantages and limitations of the procedures as compared to similar planar studies, data acquisition and computer processing.

THALLIUM-201 SPECT IMAGING

Single photon emission computed tomography (SPECT) offers several distinct advantages over other thallium imaging and planar techniques (*1*). SPECT produces a cross-sectional image by back-projection of multiple planar images which allows visualization of every wall of the heart. The reconstructed transverse slices can then be reoriented in any desired oblique plane, which is particularly important in the case of the heart because it does not lie entirely within any one plane, nor entirely parallel to or perpendicular to any of the body's anatomic planes.

The acquisition and processing of tomographic images requires a special rotating detector head and sophisticated computer software. In its current technology, SPECT is demonstrably superior to planar imaging in both sensitivity and specificity (*1-3*). Its principle limitation is decreased image resolution which is caused by the increased distance from the collimator to the body. In addition, an adequate attenuation correction for the human thorax has yet to be developed.

Patient Preparation

Patients are routinely monitored during exercise with a twelve-lead EKG. Electrodes are placed on the patient's chest after preparing the skin with methyl alcohol and extra-fine sandpaper. This preparation improves electrical contact with the skin and allows the electrode to adhere more firmly. An intravenous line consisting of a 20-gauge catheter, extension tubing, and normal saline sufficient to maintain patency throughout the exercise test is placed into an arm vein. For patients with difficult veins, a butterfly injection unit is suitable provided an arm board is used or the injection site is chosen away from a joint that will bend during exercise. A catheter, however, is preferable because it allows greater freedom of movement without extravasation. The extension tubing used should have an injection port close to the vein but not so close as to make injection difficult because of patient motion at peak exercise.

The patient's blood pressure is taken both supine and erect, a baseline 12-lead EKG is taken, and exercise is commenced using the Bruce treadmill protocol. The physician monitoring the exercise test should know the patient's medical history and current medications. Many patients with known coronary artery disease are taking nitrates or are on beta blockade, which may affect the exercise endpoint.

The patient is exercised to one or more definite endpoints (i.e., typical angina, profound fatigue, 100% target heart rate, claudication, or ST-wave changes above a certain threshold magnitude). The ^{201}Tl dose (recommended 3.5 mCi) is injected and flushed with normal saline 30 sec-1 min before the end of exercise.

Following exercise, the patient's heart rate and EKG are allowed to stabilize before imaging is commenced. Since the redistribution time for thallium is somewhat slower than that for potassium (*4*), the time to commence imaging is not as critical as once thought. During the stress image acquisition, the intravenous line is maintained in the event that medications must be given quickly.

Data Acquisition

Various techniques for ^{201}Tl tomographic data acquisition have been tried. A 180° arc (32 increments, 40 sec, 64 × 64 matrix) beginning in a right anterior oblique position and ending in a left posterior oblique position is recommended. The following reasons for this approach are: 1) the heart is an anterior, obliquely-positioned organ and the 180° arc acquires

For reprints contact: Russell Folks, Nuclear Medicine Dept., Emory University Hospital, 1364 Clifton Rd., NE, Atlanta, GA 30322.

counts symmetrically about the long axis of the left ventricle (*1*); 2) it is desirable to have the detector as close to the chest (and the heart) as possible during the acquisition; and 3) attenuation correction is not used and a 360° acquisition may acquire poor resolution images from the right side of the body which deteriorate the reconstructed slice images (*1*).

There is always a tradeoff between the number of counts and the time necessary to acquire them. With a dose of 3.5 mCi, images of improved diagnostic quality are obtainable in about 21 min. To position the patient, the detector head should pass as close to the thorax as practicable with the arms resting on the table above the head. The arms may be moved to a more comfortable position during imaging to prevent inadvertent movement caused by discomfort, provided that they are not moved between the detector and the chest or into the detector's line of sight on the opposite side of the chest.

Computer Processing

Before the reconstruction of tomographic slices, each of the 32 planar images is corrected for uniformity using a high-count flood. This correction insures that any significant count variation is a reflection of thallium localization in the myocardium as opposed to nonuniform detection by the camera-computer system. Filtered back-projection techniques are then used to generate transaxial (cross-sectional) slices through the body at the heart level. This technique is accomplished on the computer by selecting one of the left anterior oblique planar images and placing cursors above and below the heart to define the area where transaxial reconstruction occurs. During reconstruction, the images are filtered using a 1-2-1 Y-filter, which smooths the planar images in the y-direction, perpendicular to each slice, as well as a Ramp-Hanning filter with a 0.5 cutoff frequency.

It should be emphasized that these transaxial slices (Fig. 1) are perpendicular to the long axis of the body. Since the heart is oriented obliquely in the chest, other reconstructions are necessary to produce slices perpendicular to the long axis of the heart (Fig. 2). These are the tomograms that provide a three-dimensional view of the coronary vascular beds and are produced by the following operator interactions:

1. Cursors are placed through the center and on the edges of a mid-ventricular transaxial slice to define the limits for reconstruction of vertical long-axis slices (Fig. 2).
2. A mid-ventricular vertical long-axis slice is bisected with perpendicular cursors that define the limits for horizontal long-axis and short-axis slices (Fig. 3).

When the reconstructions are completed, the cursors are used to interrogate the tomographic images in the three different cardiac planes (vertical and horizontal long axis and short axis). The redistribution scan is processed in the same manner. Hence, a slice by slice visual comparison can be made of initial thallium localization and redistribution on the delayed images. Figures 4 and 5 show representative normal and ischemia hearts, respectively. Figure 6 demonstrates a persistent defect between stress and redistribution images indicating infarction.

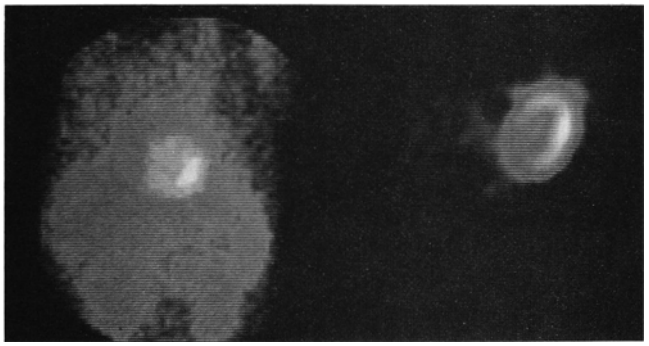

FIG. 1. Anterior planar and transaxial tomographic images are generated by backprojection with a Ramp-Hanning filter using 0.5 frequency cut-off.

Quantitative Analysis

Thallium tomographic washout kinetics are evaluated with circumferential profile algorithms similar to those used in multiple pinhole and planar imaging. The stress and redistribution short-axis slices are plotted on a maximum count per pixel basis into single images of concentric rings with the smaller apical slices in the center and the larger basal slices as the periphery (Fig. 7). These "bull's-eye" images are normalized and scaled on a color map. The stress, redistribution, and washout data (Fig. 8) are put into the bull's-eye format and compared to computer "normal" files containing data from multiple studies on patients who have no significant coronary artery disease. The results of this comparison can also be displayed using the bull's-eye format that shows the standard deviation from "normal" patients studies for stress, redistribution, and washout parameters (Figs. 8–10).

As a result of the ability to visualize the heart along its true anatomic boundaries and the enhancement of image contrast by eliminating overlapping/underlying background, the ^{201}Tl tomographic technique promotes quantitative topographic functional maps such as the "bull's-eye plot." Such quantitative analysis is preclusive with traditional planar imaging.

GATED BLOOD-POOL IMAGING

Gated single photon emission computed tomography (GSPECT) of the cardiac blood pool can be performed using a rotating gamma camera system and computer equipped with an ECG gating device. These images are acquired at each of the angular projections obtained over 30 min during a 180° or 360° rotation around the anterior chest wall. Processing time can vary, depending on resources and protocols, from 20 min–2 hr. GSPECT allows detailed assessment of regional wall motion and cardiac function without superimposition of adjacent cardiac structures that would occur with planar equilibrium gated blood-pool imaging.

Planar equilibrium radionuclide cardiac blood-pool imaging is widely accepted as a noninvasive method for assessment of cardiac performance. In using this technique, however, there is superpositioning of various cardiac structures. Only in one view, left anterior oblique of the traditional projections, can

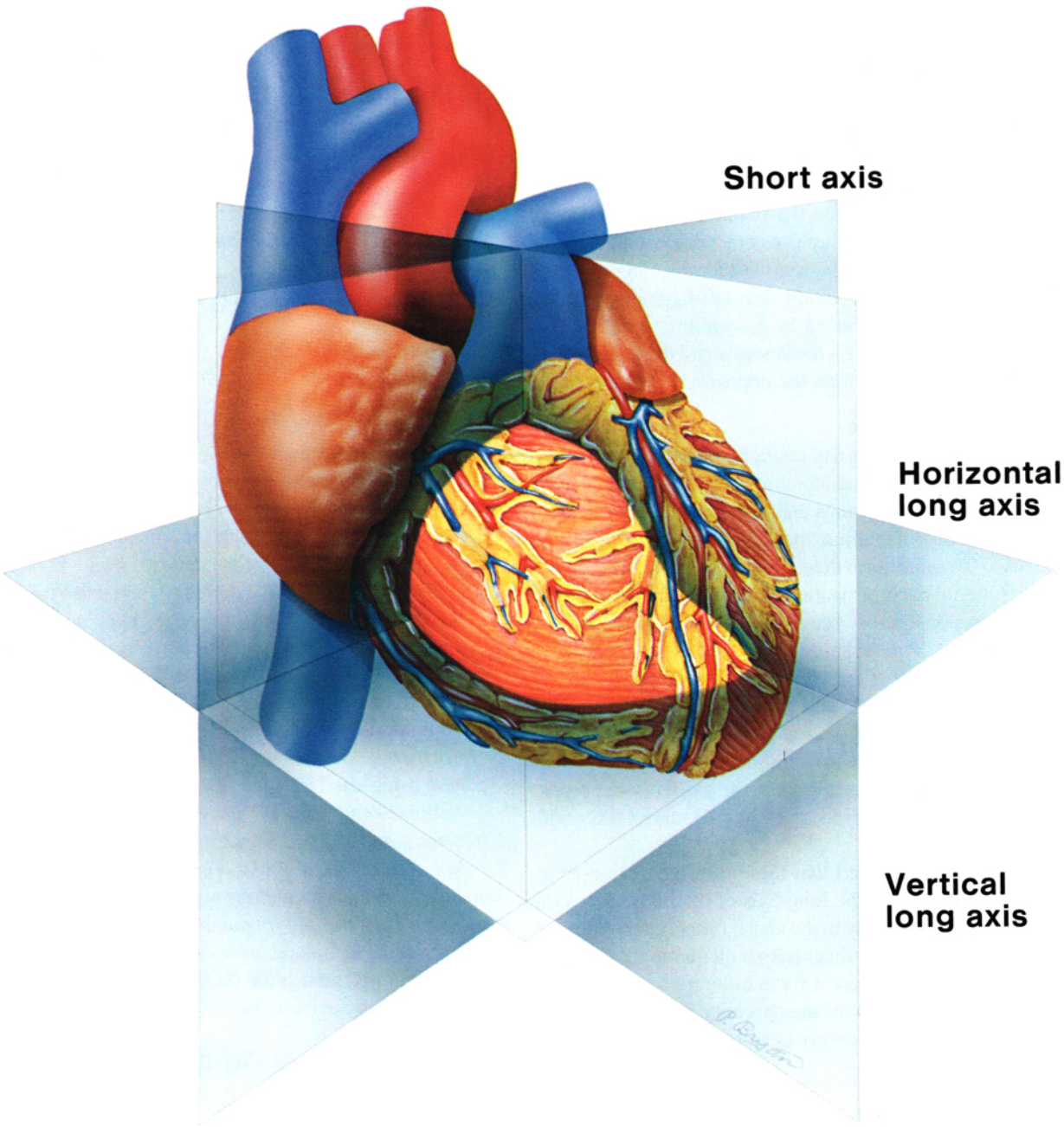

FIG. 2. Tomographic planes of the heart.

the right and left ventricle be viewed separately. Even in this view, there is superposition of different planes within the left ventricle (LV). Studies have shown that GSPECT overcomes the problems of arbitrary background correction and superposition of cardiac structures and provides a precise technique for noninvasive assessment of regional wall motion and chamber volumes both qualitatively and quantitatively (*5–10*).

Quality Control

Prior to acquisition, it is important to check camera uniformity and the system's center of rotation (COR). Most computers used for SPECT require a high-count ($\geq$30,000,000) reference flood that is stored weekly. This flood is used to correct the uniformity of the SPECT images prior to reconstruction. A lower count flood (3,000,000) should be acquired daily and corrected with the reference flood. The corrected daily flood should be uniform. Small nonuniformities are amplified by the reconstruction process, which produces severe image artifacts (*11*). Checking the physical COR of the system and the COR in the reconstruction matrix is equally

important. If there is misalignment, a loss of resolution and image artifacts will result (*12,13*). The calibration for COR should be done weekly or whenever adjustments are made to the camera or electronics. It is crucial that the reference uniformity correction flood and the COR study be acquired using the same collimator and orientation that will be used for the patient study.

FIG. 3. Transaxial and vertical reconstructed images are presented to define cursor positions for horizontal long axis and short axis.

Data Acquisition

A low-energy all-purpose collimator is used for GSPECT imaging. The patient's red blood cells are labeled and ECG electrodes are attached in a manner similar to that in conventional planar gated blood-pool imaging. At this time, most patients have a planar gated blood-pool study prior to GSPECT imaging for correlation. The patient is positioned on the tomography table with the arms raised over the head. The gantry is positioned anteriorly and the detector is lowered close to the patient's chest. The detector face must be parallel to the axis of rotation. The gantry must be rotated around the

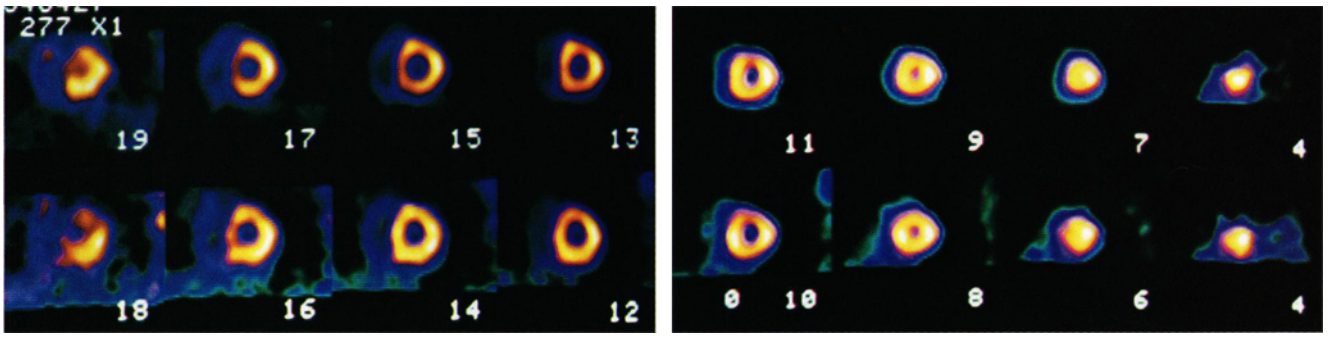

FIG. 4. Normal short-axis slices from base to apex at stress (top rows) and redistribution (bottom rows).

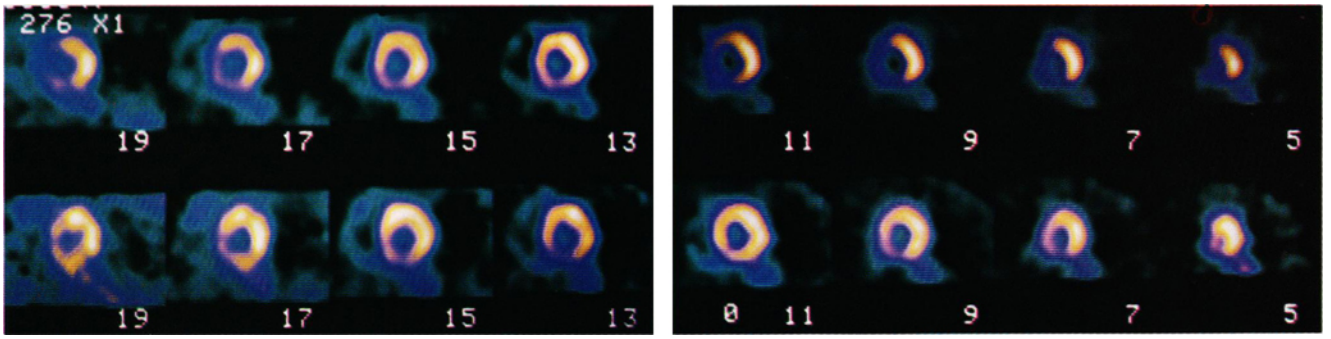

FIG. 5. Short-axis slices demonstrating myocardial ischemia involving the left descending coronary artery at stress (top row) and redistribution (bottom row).

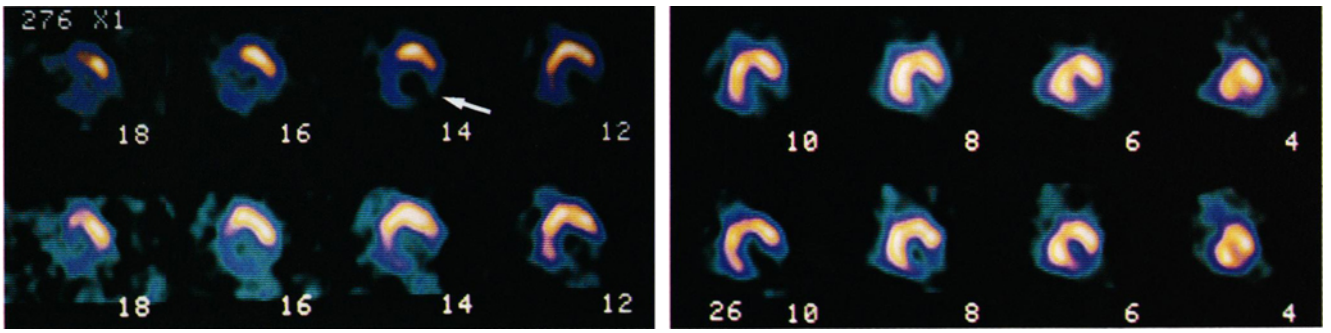

FIG. 6. Short-axis slices demonstrating an inferior wall myocardial infarction (arrow) at stress (top rows) and redistribution (bottom rows).

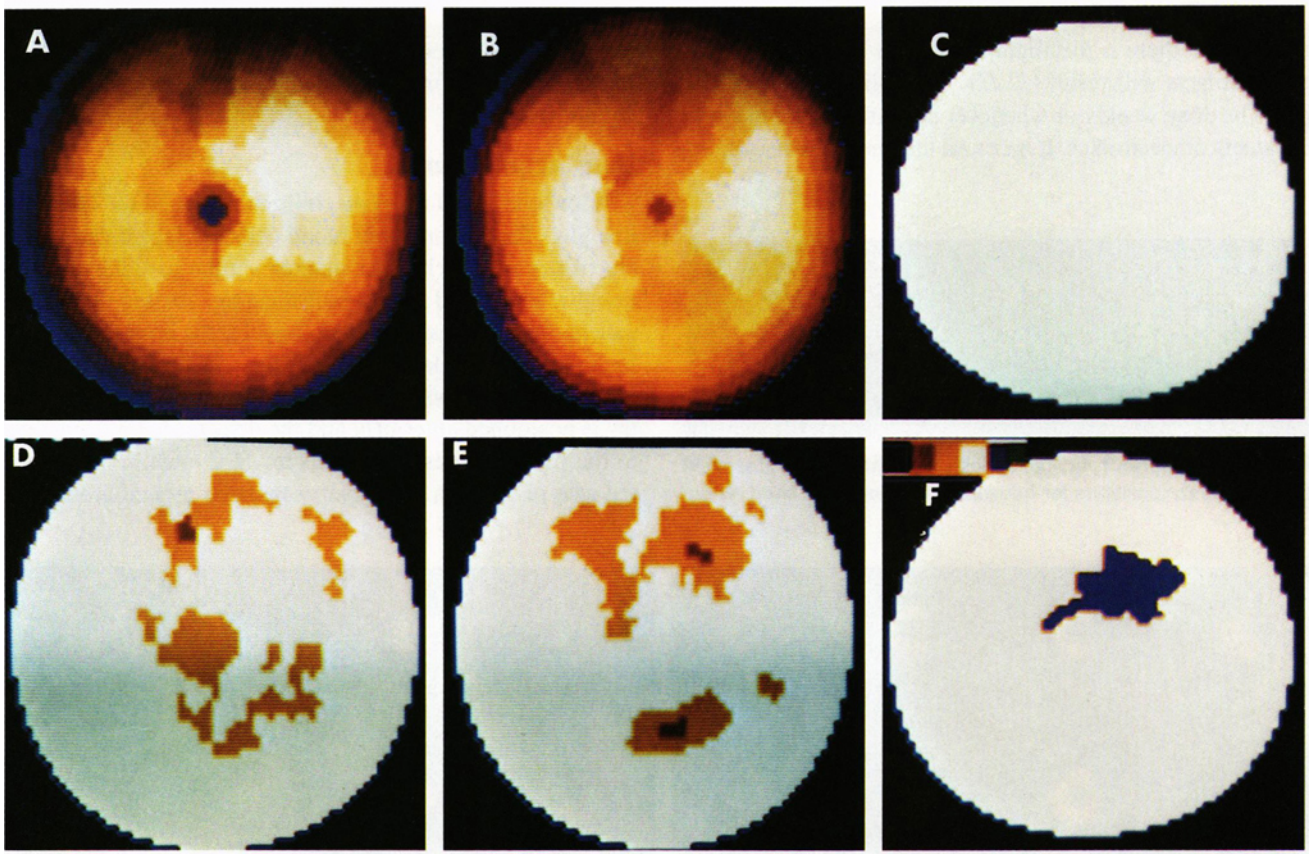

FIG. 8. Normal bull's-eye plot (see Fig. 4) is shown for stress (A), redistribution (B), washout (C), and compared to normals (D, E, F).

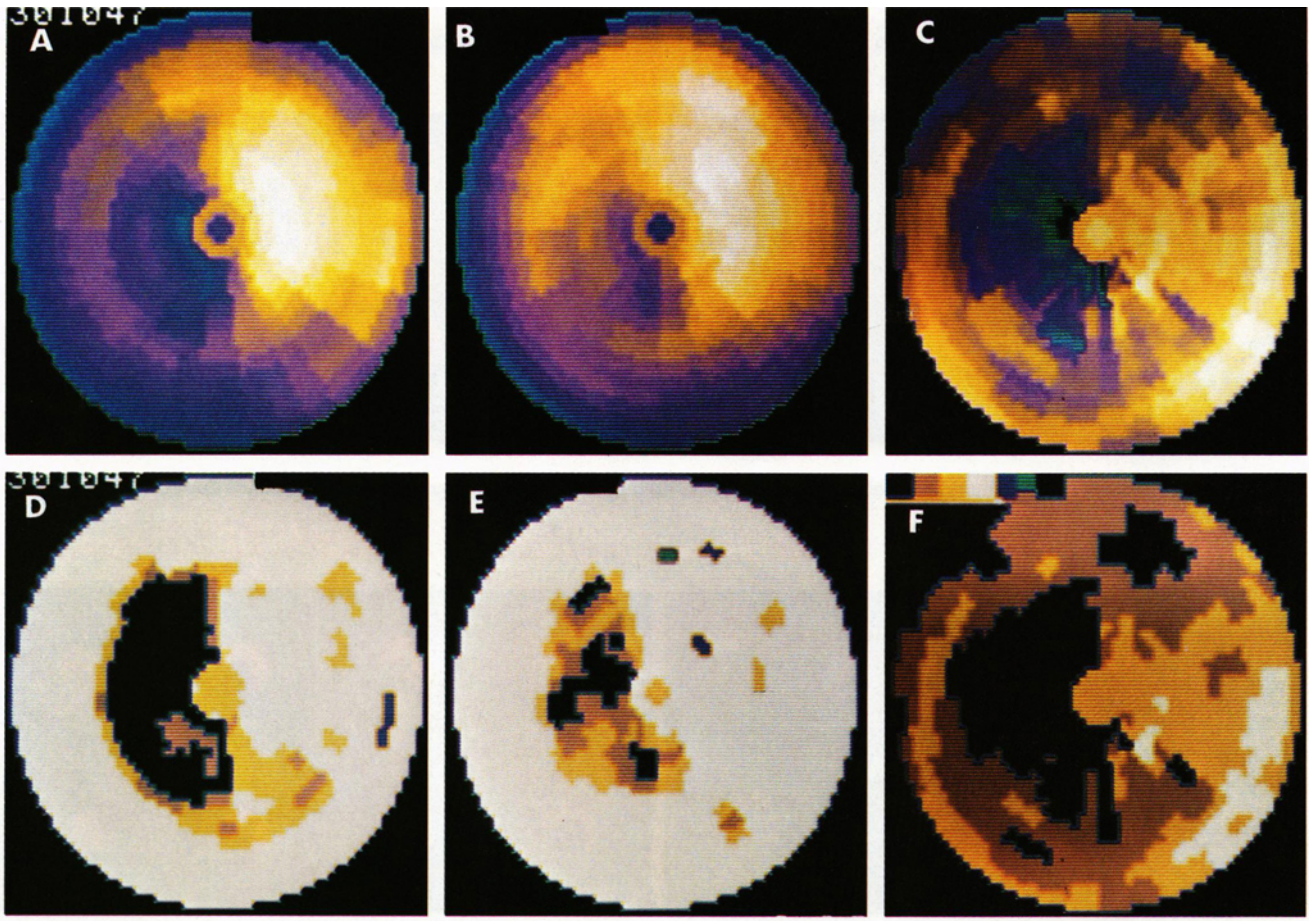

FIG. 9. Bull's-eye plot (see Fig. 5) demonstrating coronary artery disease. Perfusion defects in the septal area at stress (A), with improvement at redistribution (B), and abnormal washout (C) are compared to normals (D, E, F).

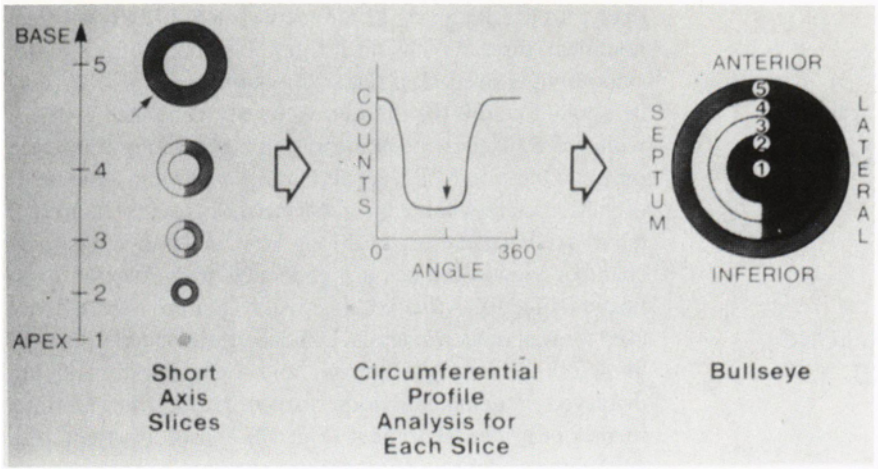

FIG. 7. Tomographic "bull's-eye plot" is a functional map of the circumferential profiles of short-axis slices from apex (center) to base (periphery).

patient to check centering of the heart in all projections without contacting the patient's shoulders and the table. If the heart moves out of the field of view, the table height is adjusted and the camera head repositioned. Most institutions acquire GSPECT images in a 180° arc beginning at 45° RAO and ending at 45° LPO. This rotation can be divided into 16, 32, or 64 equally spaced projections. A smaller angle between projections gives a clearer image with a reduction in spoke artifacts. A large angle reduces the length of acquisition time and the spoke artifacts can be reduced by using a smooth filter in reconstruction. Acquisitions through 360° give the option of selecting any 180° arc for reconstruction, but the increased imaging time is difficult for patients to tolerate unless the time per view is shortened, which decreases accumulated counts.

GSPECT images are usually acquired in a 64 × 64 matrix. Multigated images are collected at each stop using a framing

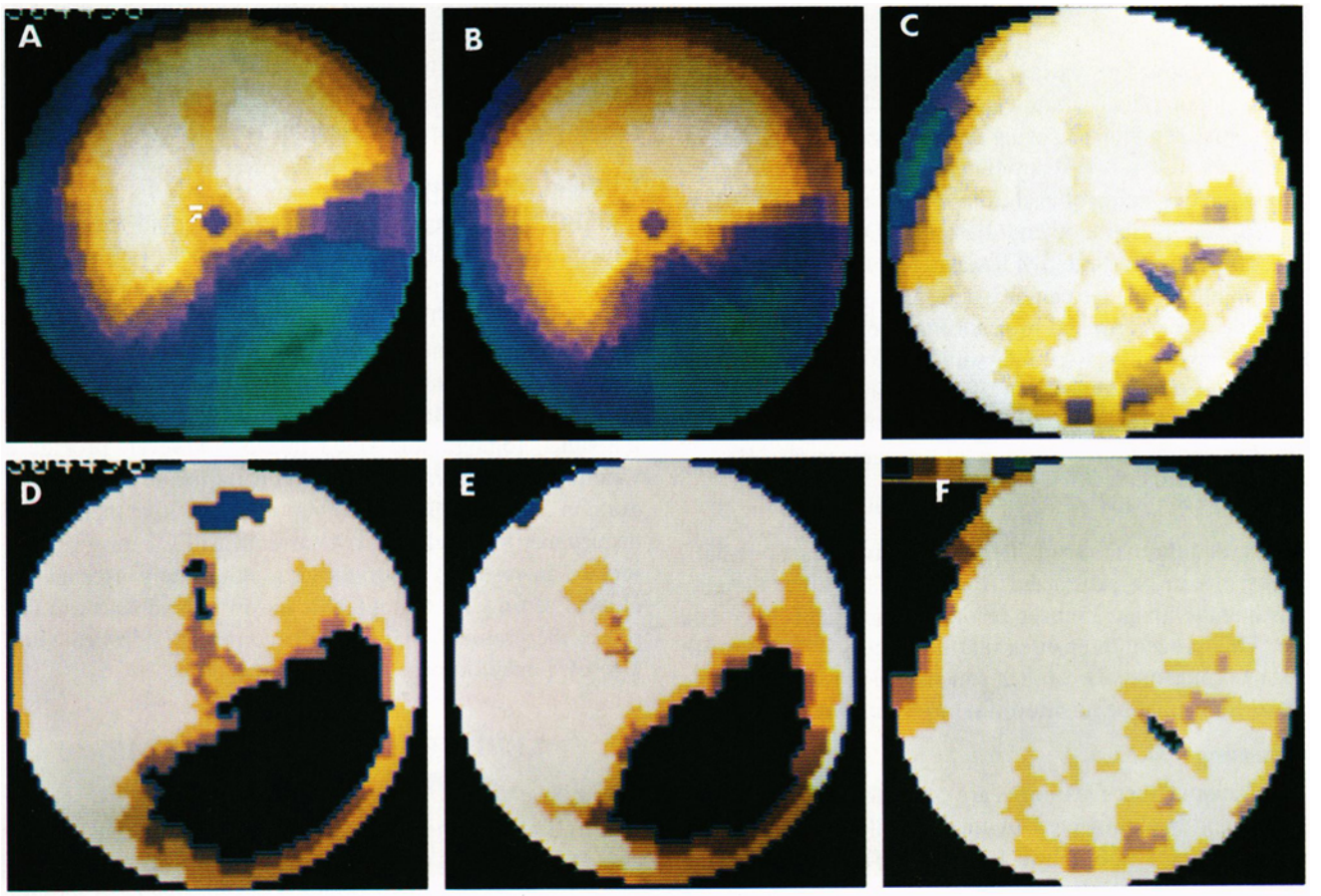

FIG. 10. Bull's-eye plot (see Fig. 6) demonstrating an inferior wall myocardial infarction. Perfusion defects in the inferobasal area at stress (A), with no improvement at redistribution (B), and normals washout (C) are compared to normals (D, E, F).

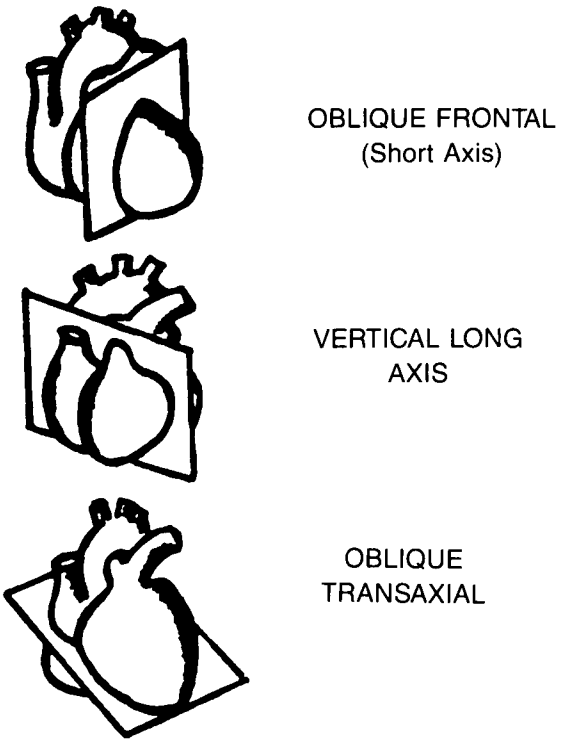

FIG. 11. Schema of the three oblique views generated from the transaxial images.

rate of 8–12 frames per cardiac cycle. If multigating capability is not available, dual gating can be used. In this case, only two images are acquired during the cardiac cycle. The image duration as well as the delay times in seconds from the R-wave to the beginning of each image must be specified. The two images correspond to end-diastole (ED) and end-systole (ES). The delay time after the R-wave to end diastole is usually negligible (0.002 sec can be used). The delay time to end-systole can be determined by recording the ECG and counting the number of 0.04-sec intervals on the ECG paper from the R-wave to the middle of the T-wave representing ES. The time to end-systole (TES) is better computed by using the following equation as described by Graham, et al. (*14*):

$$TES = 167 + 0.19 \text{ (R-R interval) msec.}$$

If an image duration time of 50 msec is desired, then one-half (25 msec) can be subtracted from the TES time, thereby recording the image 25 msec before and after calculated ES time. This procedure ensures that ES occurs within the 50 msec recording time. Because of patient discomfort, it is advisable to limit total acquisition time to 30 min or less.

Processing

After acquisition, the images are corrected for uniformity, filtered, and backprojected. A medium filter such as a 0.5 Ramp-Hanning followed by a 1-2-1 Y-filter can be used. The Y-filter smooths the planar images in the y-direction (i.e., parallel to the axis of the camera rotation), which improves the correlation between adjacent transaxial slices. Alternatively, a pure Ramp of 10 for reconstruction followed by a nonlinear three-dimensional filter may be used. If more smoothing is needed, a linear three-dimensional filter may be applied before the oblique views are generated. A slice width of 1 pixel is recommended for generating transaxial images. One-pixel width equals 6 mm if a 390-mm large-field-of-view camera when a 64 × 64 matrix is used. The frontal (short axis), sagittal (vertical-long axis), and transverse (four-chamber view) obliques are generated from the transaxial images (Fig. 11). A 2-pixel slice width (12 mm) is commonly used for wall motion analysis. Oblique views are typically used to assess ventricular function and wall motion and are displayed in a cinematic loop or recorded on film. Oblique images of a normal subject (Fig. 12) and of a patient with anteroapical akinesis (Fig. 13) are shown.

A GSPECT study, acquired by using 16 projections and dual gating of ED and ES, results in 32 images to reconstruct that require 6–8 min processing time without an array processor. It takes 14–16 min to generate the oblique images from the transaxial slices. An additional 15 min may be needed to create a display of the images on film. A GSPECT study, acquired by using 64 projections with 10-frame multigating per cardiac cycle, results in 640 images to reconstruct and greatly increased processing time. Ten minutes of processing time has been reported using 16-ED and 16-ES images to generate one set of slices orthogonal to the transverse images (*6*). In addition, quantitative analysis of LV function, volumes, and wall motion has been described using geometric or count based methods (*8–10*). Presently, much of the data reported on GSPECT are processed using software developed in research laboratories and are not generally commercially available.

Clinical Significance

GSPECT imaging of the cardiac blood pool may permit more precise evaluation of cardiac function than conventional planar imaging by overcoming the problems of superimposed cardiac structures. Three-dimensional assessment is possible by generating oblique views from transaxial images.

Practical disadvantages of GSPECT imaging as compared to planar imaging are patient discomfort and lengthy processing time. Tomographic gated images, however, provide a wealth of detailed information which may be difficult to integrate in a meaningful clinical report. Innovative methods of display may be developed, but current GSPECT imaging performed in research laboratories is not widely used in the clinical setting. As tomographic hardware and software improve, the problems stated may become less significant and GSPECT may become a routine procedure.

LEFT VENTRICULAR VOLUME DETERMINATION

SPECT imaging is a particularly powerful approach in the measurement of left ventricular volume (LVV) because transaxial images eliminate the problem of superimposed activity and make background subtraction unnecessary. It is also possible to identify the extent of the LV more exactly than in planar

images. Two approaches are used: 1) the geometric method, in which the volume is calculated from the number of voxels found in the LV; and 2) the count-based method, in which the total count in the LV is divided by the counts per ml determined in the center of the LV. The latter approach, which seems to be more accurate and reproducible, is described in detail.

When the volume of blood in the left ventricle is known, many aspects of cardiovascular physiology can be determined. Cardiac output can be calculated by subtracting the end-systolic volume (ESV) from the end-diastolic volume (EDV) and then multiplying by heart rate. The best measure of myocardial contractility is the product of end-systolic volume and end-systolic pressure (*15*). This measurement, unlike ejection fraction, is independent of preload and afterload. When combined with right ventricular data, absolute valvular regurgitation volume can be calculated.

Several techniques have been used to measure left ventricular volume. Planar radionuclide gated blood-pool imaging is being used in many nuclear medicine departments. Geometric calculations, based on the planar LV area seen on the RAO (*16*) and LAO (*17*) projections can be used to determine LVV. Calculations are also made by dividing the counts over the LV by the counts per ml of blood (*18,19*). There are major problems in appropriate background subtraction and attenuation correction with these techniques that have not been completely solved. First-pass techniques, based on geometric assumptions about the shape of the ventricle, have been used to determine LVV (*20,21*), but these methods are found to be less accurate than gated blood-pool methods (*22*).

Cardiac angiography, regarded by many as the standard for LVV determination (*23*), is an invasive procedure with several limitations and assumptions. Angiographic methods use geometric equations that are based on the assumption that the left ventricle is an ellipsoid, but this assumption is invalidated in patients with regional wall motion dysfunction (*24*). Other problems which make angiographic methods less accurate are the necessary sedation of the patient and the physiologic changes that the heart undergoes during the catheterization procedure (*25*). In addition, the injection of contrast material can alter the volume loads on the heart, and the use of sedatives during the exam can alter the physiologic resting state of the

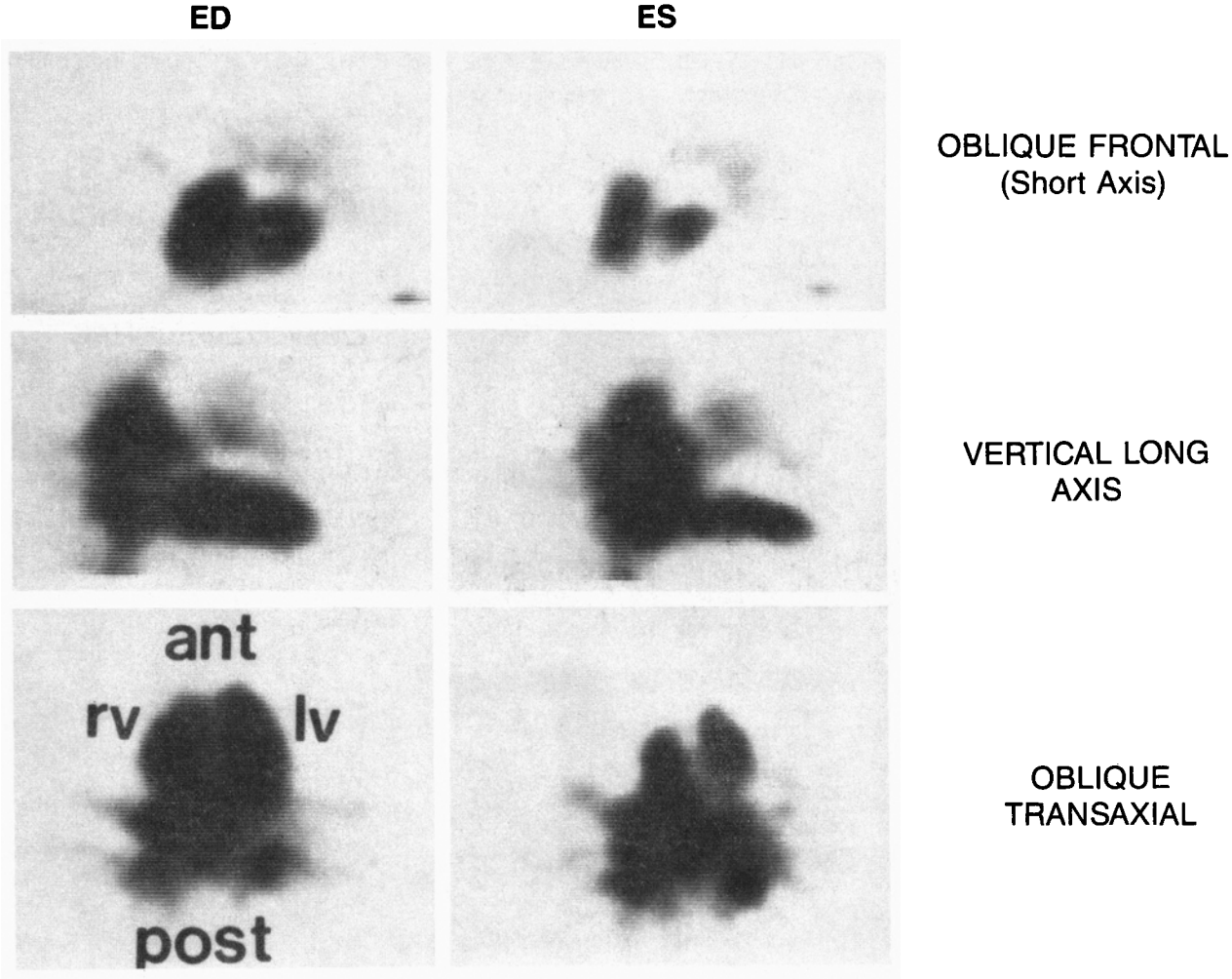

FIG. 12. Dual gated GSPECT oblique mid-ventricular slices (12 mm thick) of a normal heart. ED = end diastole, ES = end systole, Ant = anterior, Post = posterior.

heart. This procedure is invasive and not recommended for serially studying the patient's response to treatment.

The following description of a count-based nongated SPECT technique for LVV determination is a direct extension of earlier work validating the technique with phantoms (*25*).

Basic Concepts

A unique property of SPECT is its ability to display three-dimensional information of organ systems. The computer reconstructed data are displayed in tomographic slices, with individual picture elements called voxels. The volume of a voxel is measured using calibration images. Thus, the counts per ml can be calculated. If the organ radioactivity is homogeneous, as is the blood within the LV cavity, then one approach to total volume measurement is to divide the total counts in the organ by the counts per ml in the center of the organ.

To determine the size of a voxel, a set of reference point sources should be imaged tomographically using the same matrix size as that in patient studies. By plotting the counts as opposed to pixel numbers, an accurate determination of the exact location of each point source can be made. From this data it is possible to accurately calibrate the size of the pixel in cm.

After acquiring and reconstructing the tomographic study, regions of interest (ROIs) must then be drawn around the left ventricle for each tomographic slice in which the ventricle appears (Fig. 14). The counts from each slice are recorded and added to determine the total counts in the ventricle. One of the most difficult aspects of processing these studies is the creation of the ROIs around the ventricle. By stepping through the tomographic slices in figure 14, it becomes apparent that the identification of the mitral valve plane is somewhat subjective. Through heart models and echocardiographic studies, it is generally found that the mitral valve plane is perpendicular to the intraventricular septum. Of course, there are exceptions to this observation. Viewing the slices in a cinematic format also aids in the identification of the mitral valve plane. With oblique angle reorientation currently available in most tomographic software, reorienting the images might improve the mitral valve plane separation (*17*).

Activity concentration is measured by placing a voxel in the center of the ventricle (Fig. 15). The placement of the voxel is an essential step in this technique. If the voxel is closely placed to the wall of the ventricle, an underestimation of the counts/ml will be made, and therefore the LVV will be overestimated. It is also important to make the voxel the correct size. If the voxel is too large, the edge of the ventricle will be sampled and therefore overestimate the LVV. If the voxel size is too small, inadequate statistics will be recorded and errors will be introduced into further calculations. Using a 64 × 64 matrix size, without zoom, we have found the optimum size of the voxel to be 2 pixels × 2 pixels for a tomographic slice.

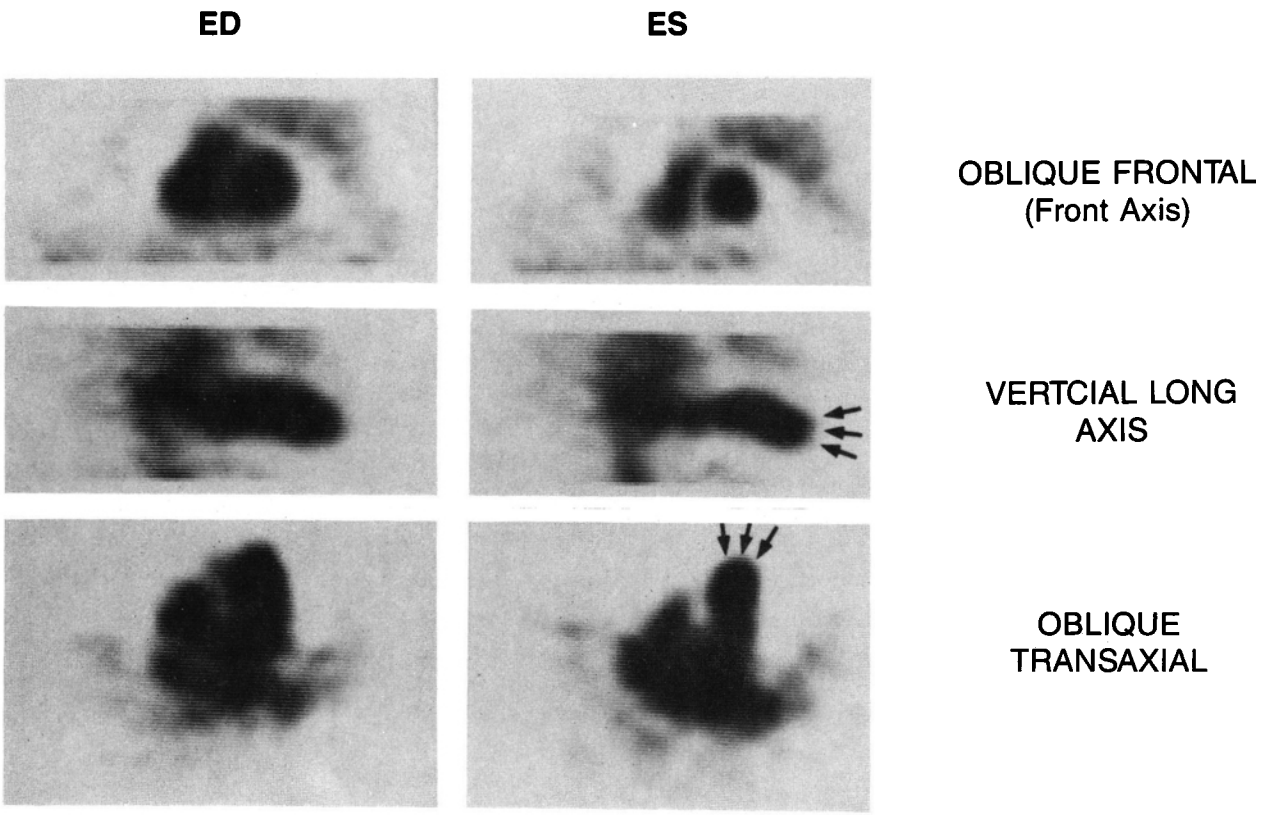

FIG. 13. Dual gated GSPECT oblique mid-ventricular slices (12 mm thick) of a patient with anteroapical akinesis. Arrows indicate area of akinesis.

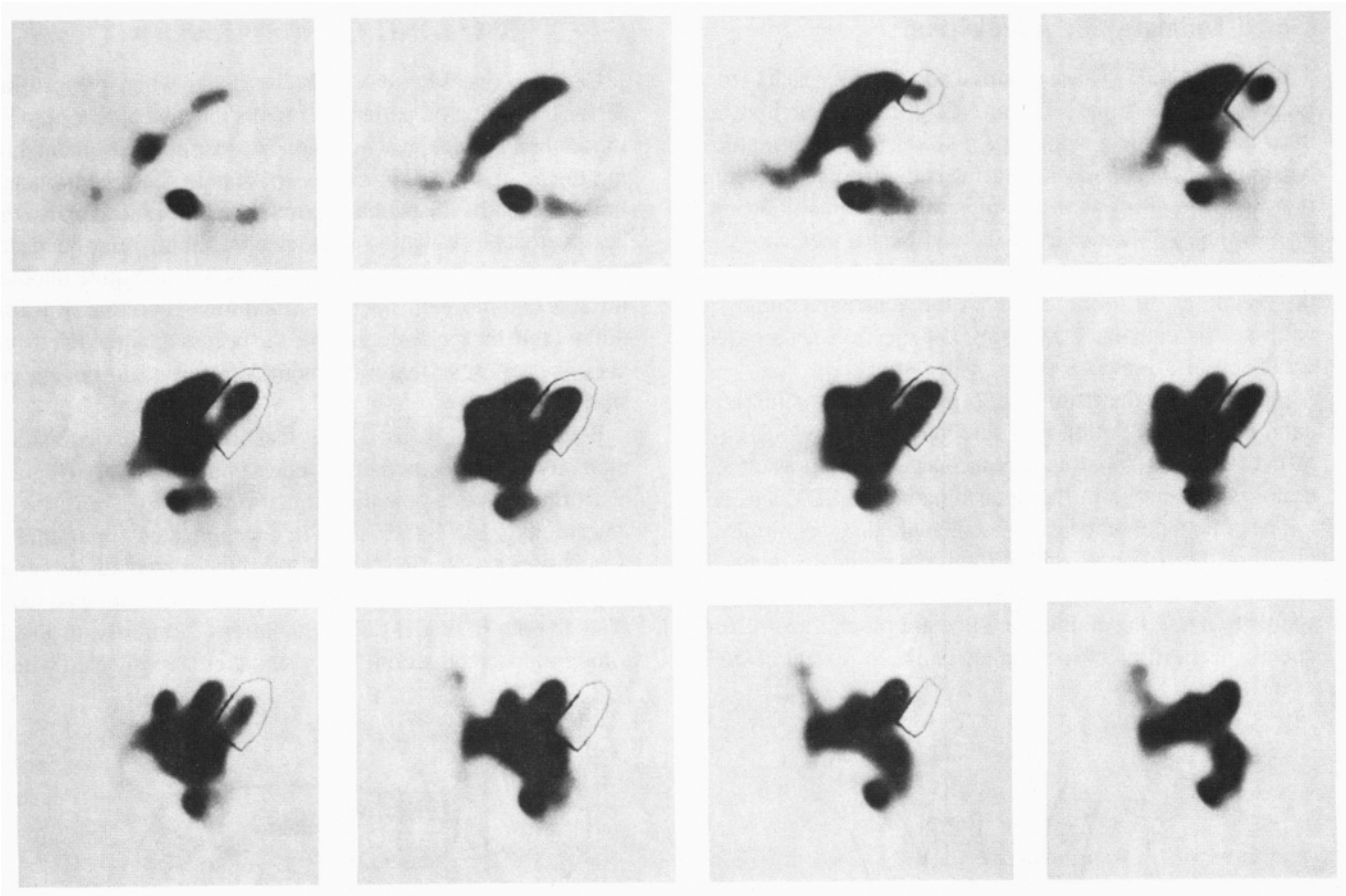

FIG. 14. Reconstructed apex to base transaxial slices through the heart with left ventricle drawn in with a light pen. The mitral valve plane is approximated by a line drawn perpendicular to the intraventricular septum.

Another method for determining the volume of blood in the ventricle is the addition of the number of voxel elements that make up the ventricular cavity. Having determined voxel size from earlier calibration, organ volume is easily obtained. Previous phantom studies illustrate that application of a certain threshold in edge detection achieves accurate volume determination (*26*). This method is known as the geometric-based approach.

In comparing the count-based method to the geometric-based method by phantom studies, Graham, et al. (*10*) found the most accurate method to be the count-based approach. Errors of the geometric method stem from the difficulty in identifying the organ edge. If this method is attempted, it is essential that it be performed with a reproducible edge-finding algorithm. Manual definition of areas will almost always result in an overestimation of volume. This method is particularly difficult.

Nongated Tomographic Acquisition

We have examined a method using the time-activity curve from a gated planar study to derive EDV and ESV. After in vitro labeling of the patient's blood with ^{99m}Tc, a standard planar gated study was performed. Sixteen frames were acquired during the cardiac cycle and a time-activity curve was created over the left ventricle using variable ROIs. The time-activity curve was used to determine the end-diastolic count to mean count ratio. Similiarly, the end-systolic count to mean count ratio was also determined. These ratios were then used to multiply the mean LVV determined by the tomographic method to calculate EDV and ESV, respectively.

Upon completion of the gated planar study, a tomographic acquisition was performed by acquiring data over 360°, 128 stops at 10 sec per stop for a total imaging time of 22 min. The patient was positioned prone with the arms placed above the head. Images were spatially smoothed, and tomographic reconstruction was performed using a Butterworth filter—cut-off frequency 0.5/pixel and filter order 5 to the data set. To check x-axis offset, a point source was tomographically acquired daily. The total time involved in acquiring and processing the LVV study was approximately 1.5 hr.

In assessing the accuracy of this technique for EDV and ESV determination, the SPECT results of 30 patients were compared to those determined by angiography. These patients were studied angiographically within 4 hr after the tomographic study. The results indicated good correlation with angiographic data ($R = 0.89$, SEE = 24 ml). Intra-observer variability was also determined ($R = 0.93$, SEE = 16 ml). Based on these comparisons, we feel that this method is indeed an accurate and reproducible technique for volume determinations of the left ventricle.

Gated Tomographic Acquisition

Bunker, et al. (*28*) have reported another approach to tomographically determine EDV and ESV. In this method, a 50 msec end-diastolic window was used during tomographic acquisition to collect data only during end-diastole. The acquisition was over 180°, with 30 stops for an acquisition time of 30 min. The EDV is determined directly from the tomographic data by determining the counts in the LV in each slice and the count per ml in the center of the ventricle. End-systole volume was calculated by using the ejection fraction (EF) results from a previous planar gated study.

In comparing the results of 25 patients with angiographic data, a good correlation is observed (R = 0.969, SEE = 23 ml). The results from this approach again show how effective tomography can be in the determination of EDV and ESV.

The advantages of the gated method are that the mitral valve plane is easier to identify and EDV is determined directly. The disadvantages are that special software is needed for the gated acquisition and the counts per slice are much lower. Consequently, it is difficult to accurately define the extent of the LV.

IMAGING CONSIDERATIONS

Certain considerations must be made when performing SPECT imaging on patients. Patients must be able to remain motionless during the acquisition because any movement during the acquisition will create artifacts in the reconstructed images. Ideally, the patient's arms should be placed above the head so that an evaluation of shoulder flexibility may be made. Patients with arthritis and bursitis may become quite uncomfortable and move during the acquisition. Therefore, it is important that the technologist take the necessary steps to ensure patient comfort so that movement does not occur during the study.

Because gating is used in at least one type of acquisition modality with both methods, studies of patients with irregular heart rates poses a potential limitation of SPECT imaging in determining EDV and ESV. In the nongated tomographic acquisition, problems arise in finding the correct ratio of end-diastolic counts to mean counts, which would then lead to an error in both EDV and ESV calculations. Similarly, in gated-tomographic acquisition, fewer statistics are collected which

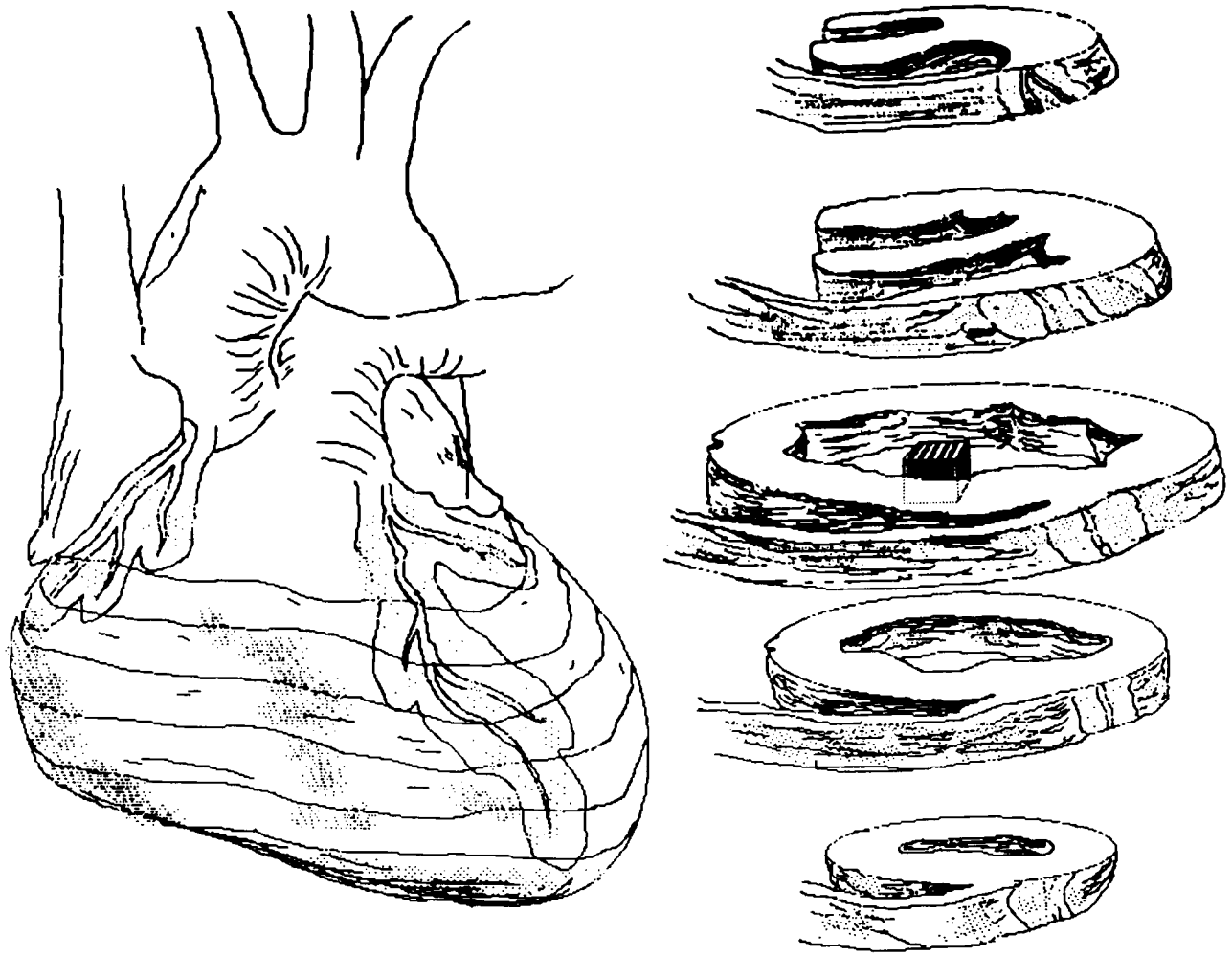

FIG. 15. The concentration in cts/unit volume is determined by placing a voxel in the center of the LV. This value is then used for LVV determination.

results in a larger source of error in volume determination.

Another consideration of tomographic imaging of the heart is the choice between 180° and 360° acquisitions. In a teaching editorial by Hoffman (*27*), the advantages of 360° and 180° imaging are discussed. When imaging ^{99m}Tc, 360° imaging is suggested as the method of choice. However, similar results from our laboratory and the work by Bunker, et al. (*28*) indicate that the differences between 360° and 180° acquisitions are small when imaging the heart. One possible explanation for this factor is that the heart is not centered in the chest cavity. Sufficient information can be obtained by simply imaging 180° from the LPO to RAO position.

In conclusion, measurement of the volume of blood in the left ventricle is important in the assessment of cardiovascular physiology. SPECT has been shown to be an accurate method for LVV measurement. Attenuation and background problems are no longer a factor, and geometric assumptions are not required. This technique should make it possible to follow patients before and after treatment.

ACKNOWLEDGMENT

Russell Folks and Lawrence Banks wish to thank Jane Lanier for her dedicated efforts throughout the several revisions of this manuscript. This work was supported in part by a grant from Du Pont/New England Nuclear, Medical Products, North Billerica, MA.

REFERENCES

1. Ritchie JL, Williams DL, Harp G, et al. Transaxial tomography with thallium-201 for detecting remote myocardial infarction; Comparison with planar imaging. *Am J Cardiol* 1982;50:1236-41.

2. Prigent F, Friedman J, Maddahi J, et al. Comparison of rotational tomography with planar imaging for thallium-201 stress myocardial scintigraphy. *J Nucl Med* 24:No. 5, P 18, 1983 (abst).

3. Ritchie JL, Larson SM, Israelson A, et al. Thallium-201 imaging: A comparison of single photon emission computed tomography and planar imaging employing a standard heart phantom. *Am J Cardiol* 1980;45:464, (abst).

4. Serafini A, Gilson A, Smoak W, eds. *Nuclear Cardiology*, New York, Plenum Co., 1977.

5. Moore ML, Murphy PH, Burdine JA. ECG-gated emission computed tomography of the cardiac blood pool. *Radiology* 1980;134:233-35.

6. Maublant J, Bailly P, Mestas D, et al. Feasibility of gated single photon emission transaxial tomography of the cardiac blood pool. *Radiology* 1983;146:837-39.

7. Tamaki N, Mukai T, Ishii Y, et al. Multiaxial tomography of heart chambers by gated blood-pool emission computed tomography using a rotating gamma camera. *Radiology* 1983;147:547-54.

8. Corbett JR, Jansen DE, Lewis SE, et al. Gated blood pool transaxial tomography: Left ventricular volumes and ejection fraction. *J Am Coll Cardiol* 1984;3:590 (abst).

9. Barat JL, Brendel AJ, Colle JP, et al. Quantitative analysis of left-ventricular function using gated single photon emission tomography. *J Nucl Med* 1984;25:1167-74.

10. Graham MM, Caputo GR. Measurement of left ventricular volume using emission computed tomography. In *Emission Computed Tomography Current Trends*, Esser PD, ed., New York, The Society of Nuclear Medicine, 1983, pp 147-53.

11. Rogers WL, Clinthorne NH, Harkness BA, et al. Field-flood requirements for emission computed tomography with an Anger camera. *J Nucl Med* 1982;23:62-68.

12. Areeda J, Chapman D, Van Train K, et al. Methods for characterizing and monitoring rotational gamma camera system performance. In *Emission Computed Tomography Current Trends*, Esser PD, ed., New York, The Society of Nuclear Medicine, 1983, pp 81-90.

13. Jaszczak RJ, Greer K, Coleman RE. SPECT system misalignment: Comparison of phantom and patient images. In *Emission Computed Tomography Current Trends*, Esser PD, ed., New York, The Society of Nuclear Medicine, 1983, pp 57-69.

14. Graham M, Cavailloes F, Ritchie JL, et al. Performance characteristics of a commercial ECG gate. *J Nucl Med* 1980;21:387-90.

15. Grossman W, Braunwald E, Mann T, et al. Contractile state of the left ventricle in man as evaluated from end-systolic pressure-volume relations. *Circulation* 1977;56:845-52.

16. Sullivan RW, Bergeron DA, Vetter WR, et al. Peripheral venous scintillation angiography in the determination of left ventricular volume in man. *Am J Cardiol* 1971;28:563-67.

17. Uren RF, Newman HN, Hutton BF, et al. Geometric determination of left ventricular volume from gated-pool studies using a slant hole collimator. *Radiology* 1983;147:541-45.

18. Links JM, Becker LC, Shindledecker JG, et al. Measurement of absolute LVV from gated blood pool studies. *Circulation* 1982;65:82-91.

19. Dehmer GJ, Lewis SE, Hillis LD, et al. Nongeometric determination of left ventricular volume from equilibrium blood-pool scans. *Am J Cardiol* 1980;45:293-300.

20. Ashburn W, Kastu KW, Karliner J, et al. Left ventricular ejection fraction and volume determinations by radionuclide angiography. *Semin Nucl Med* 1973;3:165-76.

21. Ishii Y, MacIntyre WJ. Measurement of heart chamber volumes by analysis of dilution curves simultaneously recorded by scintillation camera. *Circulation* 1971;44:37-46.

22. Massie BM, Kramer BL, Gertz EW, et al. Radionuclide measurement of LVV: Comparison between geometric and count-based methods. *Circulation* 1982;65:725-30.

23. Dodge HT, Sandler H, Ballew DW, et al. The use of biplane angiocardiography for the measurement of left ventricular volume in man. *Am Heart J* 1960;60:762-76.

24. Hillis LD, Winniford MD, Dehmer GJ, et al. Left ventricular volumes by single-plane cineangiography: In vivo validation of the Kennedy regression equation. *Am J Cardiol* 1984;53:1159-63.

25. Vine DL, Hegg TD, Dodge HT, et al. Immediate effect of contrast medium injection on left ventricular volumes and ejection fraction: A study using metallic epicardial markers. *Circulation* 1977;56:379-84.

26. Tauxe WN, Soussaline F, Todd-Pokropek A, et al. Determination of organ volume by single photon emission tomography. *J Nucl Med* 1982;23:984-87.

27. Hoffman EJ. 180° compared with 360° sampling in SPECT. *J Nucl Med* 1982;23:745-47.

28. Bunker SR, Hartshorne MF, Schmidt WP, et al. Left ventricular volume determination from single photon emission computed tomography. *Am J Radiol* 1985;144:295-98.